INTERNATIONAL JOURNAL OF ADAPTIVE CONTROL AND SIGNAL PROCESSING
Int. J. Adapt. Control Signal Process. 2001; **15**:353–375 (DOI: 10.1002/acs.671)

Supervisory field-oriented control of induction motors with uncertain rotor resistance

G. W. Chang[1], J. P. Hespanha[2], A. S. Morse[3], M. S. Netto[4] and R. Ortega[4,*,†]

[1] *Vetrotex International, Groupe Saint-Gobain, 767, quai des Allobroges, 73009, Chambéry, France*
[2] *University of Southern California, Electrical Engineering – Systems, 3740 McClintock Avenue, Room 318, Los Angeles, CA 90089-2563, U.S.A.*
[3] *Center for Computational, Vision and Control, Yale University, New Haven, CT 06520, U.S.A.*
[4] *Lab. des Signaux & Systèmes, CNRS–Supélec–Univ. Paris Sud, Plateau de Moulon, 91192 Gif sur Yvette, France*

SUMMARY

It is well known that the performance of the (industry standard) field-oriented control (FOC) for induction motors is highly sensitive to uncertainties in the rotor resistance. In this paper we describe how to use supervisory control to obtain an adaptive implementation of FOC for current-fed machines. The unknown rotor resistance is assumed to belong to a discrete set, while the uncertain load torque ranges in a given compact set. Even though no restrictions are *a priori* imposed on the size of these sets, their definitions reflect the prior knowledge of the designer, which is effectively incorporated in the supervisory control algorithm. The supervisor selects from these sets values for the parameters to be applied to the FOC, a choice that is made by continuously comparing suitably defined performance signals. We prove that the proposed supervisor achieves *global stabilization* of the system when the load torque is known to belong to a given finite set of values. Apparently, this is the first globally convergent adaptive algorithm for current-fed machines which simply adds adaptation to the widely popular FOC and is not a radically new complicated controller, hence it is more likely to be adopted by practitioners. Some simulation results illustrate the properties of the algorithm. Copyright © 2001 John Wiley & Sons, Ltd.

KEY WORDS: supervisory control; indirect field-oriented control; induction motors

1. INTRODUCTION AND PROBLEM FORMULATION

In most practical applications, induction motors are operated in the so-called current-fed mode. The behaviour of the machine in this operation mode is described by a third-order model which expresses the rotor flux $\lambda \in \mathbb{R}^2$ and the stator currents $u \in \mathbb{R}^2$ in a reference frame rotating at the

* Correspondence to: R. Ortega, Lab. des Signaux and Systèmes, CNRS-Supélec-Univ. Paris Sud, Plateau de Moulon, 91192 Gif sur Yvette, France.
† E-mail: rortega@lss.supelec.fr

Contract/grant sponsor: CAPES

rotor angular speed ω as

$$\mathrm{P}: \begin{cases} \dot{\lambda} = -R\lambda + Ru \\ \dot{\omega} = \tau - \tau_{\mathrm{L}} \\ \tau = u^{\mathrm{T}} \mathscr{J} \lambda \\ \beta = |\lambda| \end{cases} \tag{1}$$

Here $\tau \in \mathbb{R}$ is the generated torque; $R \in \mathbb{R}$ is the rotor resistance taking values in an interval $[R_m, R_M]$, with $R_m > 0$; $\tau_{\mathrm{L}} \in \mathbb{R}$ is the load torque taking values in another interval $[\tau_{\mathrm{L}m}, \tau_{\mathrm{L}M}]$; and

$$\mathscr{J} \triangleq \begin{bmatrix} 0 & -1 \\ 1 & 0 \end{bmatrix}$$

The outputs to be regulated are ω and the rotor flux norm β. These should be driven to *constant* values ω_* and $\beta_* > 0$, respectively, while ω is the *only measurable signal*.

Without loss of generality (see e.g., References [1, 2]), we set all parameters to one except R and τ_{L}, which we assume constant but unknown. We assume known, however, sets $\mathscr{R} \subset [R_m, R_M]$ and $\mathscr{T} \subset [\tau_{\mathrm{L}m}, \tau_{\mathrm{L}M}]$ in which they range, respectively. See Reference [2] for a detailed derivation of this model from the textbook standard.

Field-oriented control (FOC) is the *de-facto* industry standard for high-performance application induction motors. In its indirect formulation FOC is a non-linear dynamic output feedback controller with a cascaded structure where the inner loop control consists of a rotation and the outer loop is typically defined via a PI regulator around the velocity error. The motor model and the FOC are depicted in Figure 1, with the FOC defined as

$$\mathbf{C}(\hat{R}): \begin{cases} u = \mathrm{e}^{\mathscr{J}\rho} \begin{bmatrix} \beta_* \\ \frac{\tau_d}{\beta_*} \end{bmatrix} = \begin{bmatrix} \cos(\rho) & -\sin(\rho) \\ \sin(\rho) & \cos(\rho) \end{bmatrix} \begin{bmatrix} \beta_* \\ \frac{\tau_d}{\beta_*} \end{bmatrix} \\ \dot{\rho} = \dfrac{\hat{R}}{\beta_*^2}\ \tau_d \\ \tau_d = -K_P \mathrm{e}_\omega - K_I v \\ \dot{v} = \mathrm{e}_\omega \\ \mathrm{e}_\omega = \omega - \omega_* \end{cases} \tag{2}$$

Here $\hat{R} > 0$ is the *constant estimated* rotor resistance, and $K_P, K_I > 0$ are tuning gains. We use the notation $\mathbf{C}(\hat{R})$ to underscore the dependence of the controller on the estimated rotor resistance. It is important to remark that, even though τ_{L} is unknown, the controller does not attempt to estimate it, since its effect is countered by the integral action, at least as long as τ_{L} remains constant.

The following remark concerning the practical implementation of FOC is in order: the angle ρ, which plays the role of an estimate of the rotor flux angle, is generated as the output of an integrator whose input τ_d converges to a non-zero constant, therefore it grows unbounded. Since ρ is subsequently used as the argument of periodic functions, the windup problem is avoided by simply resetting the integrator.

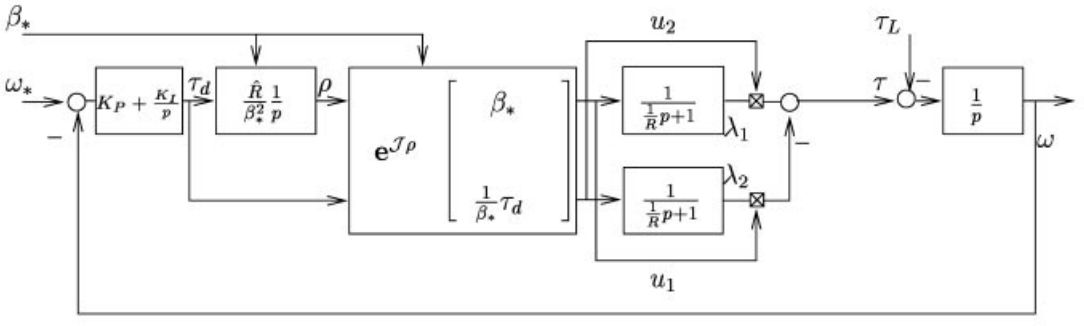

Figure 1. Current-fed induction motor with indirect FOC. Motor model presented in a frame of reference rotating with rotor electrical speed.

In Reference [1] (see also Reference [2]) we have shown that the closed-loop system (1)–(2) has a unique equilibrium point if and only if $0 < \hat{R} \leqslant 3R$. This is satisfied in most practical applications. Furthermore, we prove that this equilibrium is *globally exponentially stable* provided $|R - \hat{R}|$ is sufficiently small.‖ This establishes, via total stability arguments, that the algorithm is robustly stable *vis-à-vis* variations in the rotor resistance, which are unavoidable in practical applications. However, extensive simulation and experimental evidence, e.g., References [3–5, 2] have shown that *performance* and power efficiency are significantly degraded when there are large errors in the rotor resistance estimate. This stems from the fact that the main objective of field orientation is not achieved in this case [2].

A natural approach to solve this problem is to make the FOC adaptive by defining an update law for $\hat{R}$. In this paper we achieve this by making use of a *supervisory control* [6, 7]. To this end, we define a discrete set of candidate resistance values

$$\mathscr{R} \triangleq \{R_1, R_2, \ldots, R_N\} \subset [R_m, R_M] \tag{3}$$

with $N \geqslant 2$, and *assume* that the actual rotor resistance belongs to this set,** i.e.

$$\exists\, i_* \in \mathscr{N} \triangleq \{1, 2, \ldots, N\} : R_{i_*} = R$$

A supervisor, which selects values in $\mathscr{R}$ to be applied to the FOC, is then set in place. The supervisor (i) continuously compares suitably defined performance signals, each associated with a specific element of $\mathscr{R}$, and (ii) uses in the FOC that value in $\mathscr{R}$ that corresponds to the smallest performance signal. The rationale underlying the supervisor's operation is straightforward: the nominal model whose associated performance signal is the smallest, 'best' approximates the process behaviour and thus the corresponding controller ought to be able to control the process better. The origin of this idea is the concept of certainty equivalence. This is a well-known

‖ Bounds on the allowable estimation error in terms of K_P, K_I and τ_L are also given in that paper.

** For all practical purposes we can relax this assumption to 'R sufficiently close to a set member'. This can, of course, be ensured taking a finer grid, at the price of increased computational burden.

heuristic idea central to the whole adaptive control literature whose role has been formally established for linear plants in Reference [8] and extended to non-linear systems in the recent paper [9]. See also Reference [10].

The performance signals in supervisory control [6] are generated by designing an estimator for each member of $\mathscr{R}$ and evaluating their norm-squared output estimation error. This task is complicated in the present problem because, besides the uncertainty in R, the load torque τ_L is also unknown. Furthermore, not all state variables are available for measurement. To overcome these difficulties we need to implement a flux observer and simultaneously estimate R and τ_L. The main result of the paper is the proof that this new globally convergent adaptive observer—which is of interest on its own—together with the proposed supervisor achieves *global stabilization* of the system. Apparently, this is the first globally convergent adaptive algorithm for current-fed machines, which is, moreover, an 'add-up' to the widely popular FOC, and not a radically new complicated controller that will hardly be adopted by practitioners.

The problem of control of induction motors with uncertain rotor resistance has a long history, dating at least as far back as Reference [11]. Many papers on the industrial electronics literature have been reported on this topic. However, as discussed in Reference [12], most of these studies rely on simplifying assumptions like linearization and quasi-static operations. For current-fed machines besides the algorithm reported here, we are aware only of two other results. First, the globally convergent *estimation* algorithm of Reference [12], which contains also some interesting closed-loop experimental results. However, no proof of stability for the control problem is given in that paper. Second, we proposed in Reference [13] a sliding mode-based adaptive FOC, which is shown to be globally convergent provided the rotor resistance ranges in a *sufficiently small* set. It is somehow paradoxical that interesting theoretical solutions have already been found for the more complicated voltage-fed induction machine, see e.g. References [14, 15]. This might be explained by the fact that this model includes the stator dynamics which provides more information about the state of the machine through additional measurable signals. It should be pointed out that, except for Reference [13], all the other works cited above propose new control schemes, whose complexity is in sharp contrast with the simplicity of FOC.

The remaining of the paper is organized as follows. In Section 2 we present the supervisory control algorithm. The stability analysis of the closed loop is given in Section 3. In Section 4 we show some simulation results which illustrate the properties of the algorithm. We close the paper with some concluding remarks in Section 5. The proof of a technical lemma needed for the main result is given in the Appendix.

2. ESTIMATOR-BASED SUPERVISION

A block diagram describing the overall supervisory control system is depicted in Figure 2. It consists of the induction motor model $\mathrm{P}:(u,\tau_L)\mapsto\omega$ (described by (1)), in closed-loop with the parameterized FOC $\mathrm{C}(\hat{R}):(\omega,\omega_*,\beta_*)\mapsto u$ (with dynamics (2)), whose estimated rotor resistance $\hat{R}$ is generated by the estimator-based *supervisor* $\Sigma:(u,\omega)\mapsto\hat{R}$. We proceed now to derive the elements entering in the definition of Σ. To motivate our developments we consider first (Section 2.1) a hypothetical case of known parameters. The supervisor is derived in Section 2.2. For ease of reference we summarize the equations in Section 2.3.

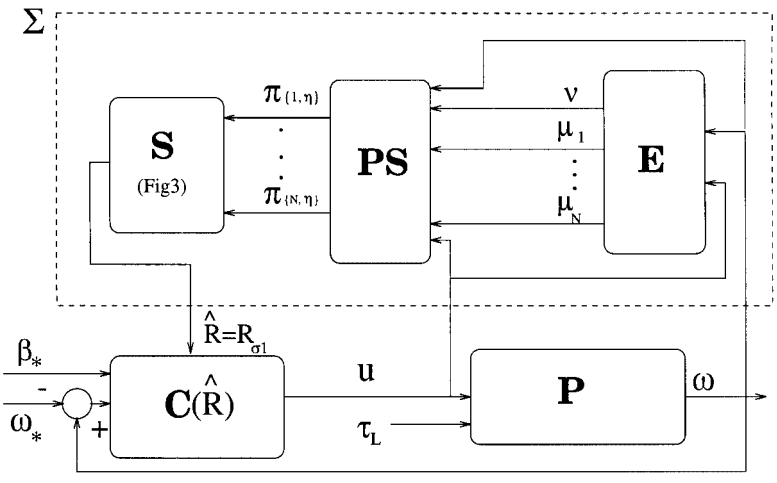

Figure 2. Configuration of the supervisory control system.

2.1. *Observer design for the known parameter case*

Assume for the moment that R and τ_L were known. In this case one could construct a nonlinear state-observer for (1) using the equations[††]

$$\dot{\hat{\lambda}} = -R\hat{\lambda} + Ru \tag{4}$$

$$\dot{\hat{\omega}} = u^T \mathcal{J}\hat{\lambda} - \tau_L - \kappa(1 + |u|^2)(\hat{\omega} - \omega) \tag{5}$$

where κ is any constant larger than $\frac{1}{2}$. In fact, with $\hat{\lambda}$ and $\hat{\omega}$ so defined, one can show that the estimation errors

$$\tilde{\lambda} \triangleq \hat{\lambda} - \lambda, \qquad \tilde{\omega} \triangleq \hat{\omega} - \omega \tag{6}$$

converge to zero exponentially fast for any piecewise continuous (possibly unbounded) input signal u. To see that this is so consider an arbitrary piecewise continuous input signal u. From (6) one concludes that

$$\dot{\tilde{\lambda}} = -R\tilde{\lambda}, \qquad \dot{\tilde{\omega}} = u^T \mathcal{J}\tilde{\lambda} - \kappa(1 + |u|^2)\tilde{\omega}$$

along solutions to (1), (4)–(5). Thus, defining the exponentially weighted Lyapunov-like function

$$V = e^{\gamma t}\left(\frac{1}{2R}|\tilde{\lambda}|^2 + \frac{1}{2}\tilde{\omega}^2\right)$$

[††] Notice that we have introduced a weighting factor $(1 + |u|^2)$ in the correction term of the observers. The role of this term will be clarified later.

where γ is a positive constant, one concludes that

$$\begin{aligned}\dot{V} &= \gamma V + e^{\gamma t}(-|\tilde{\lambda}|^2 + \tilde{\omega} u^T \mathcal{J} \tilde{\lambda} - \kappa(1+|u|^2)\tilde{\omega}^2) \\ &\leqslant \gamma V + e^{\gamma t}(-|\tilde{\lambda}|^2 + |\tilde{\omega} u|\,|\tilde{\lambda}| - \kappa(1+|u|^2)\tilde{\omega}^2)\end{aligned}$$

along solutions to (1), (4)–(5). Using the Schwartz inequality one further concludes that

$$\dot{V} \leqslant \gamma V + e^{\gamma t}(-\tfrac{1}{2}|\tilde{\lambda}|^2 - \kappa\tilde{\omega}^2 - (\kappa - \tfrac{1}{2})|u|^2\tilde{\omega}^2)$$

and therefore

$$\dot{V} \leqslant -e^{\gamma t}(\kappa - \tfrac{1}{2})|u|^2\tilde{\omega}^2 \tag{7}$$

for any positive constant γ such that

$$\gamma \leqslant \min\{R, 2\kappa\}$$

For such a γ, and since $\kappa > \frac{1}{2}$, V must then be bounded and therefore both $\tilde{\lambda}$ and $\tilde{\omega}$ converge to zero as fast as $e^{-\gamma/2t}$. Moreover, integrating both sides of (7), one further concludes that

$$\int_0^t e^{\gamma\tau}|u(\tau)|^2\tilde{\omega}^2(\tau)\,d\tau \leqslant \frac{2}{2\kappa - 1}V(0), \qquad t \geqslant 0$$

Now, for each piecewise continuous signal u, Equation (5) can be regarded as a linear time-varying system with inputs $u^T\mathcal{J}\hat{\lambda} + \kappa(1+|u|^2)\omega$ and $-\tau_L$. Thus the same estimate $\hat{\omega}$ could also be generated by the two-dimensional system

$$\dot{\mu} = -\kappa(1+|u|^2)\mu + u^T\mathcal{J}\hat{\lambda} + \kappa(1+|u|^2)\omega \tag{8}$$

$$\dot{v} = -\kappa(1+|u|^2)v - 1 \tag{9}$$

$$\hat{\omega} = \mu + \tau_L v. \tag{10}$$

We will see shortly that generating $\hat{\omega}$ as above is more convenient for our purposes. The following has been proved:

Proposition 2.1

Let γ be a positive constant no larger than $\min\{R, 2\kappa\}$. For any piecewise continuous signal u and any initial conditions there exist positive constants c_1, c_2, c_3 such that

$$|\tilde{\lambda}| \leqslant e^{-\gamma/2t}c_1, \quad |\tilde{\omega}| \leqslant e^{-\gamma/2t}c_2, \quad \int_0^t e^{\gamma\tau}(1+|u(\tau)|^2)\tilde{\omega}^2(\tau)\,d\tau \leqslant c_3, \quad t \geqslant 0$$

along solutions to (1), (4), (6), (8)–(10).

2.2. Derivation of the supervisor

The previous proposition motivates the following *multi-estimator*:

$$\begin{aligned}\dot{\lambda}_i &= -R_i\lambda_i + R_i u, && i \in \mathcal{N}\\ \dot{\mu}_i &= -\kappa(1+|u|^2)\mu_i + u^{\mathrm{T}}\mathcal{J}\lambda_i + \kappa(1+|u|^2)\omega, && i \in \mathcal{N}\\ \dot{v} &= -\kappa(1+|u|^2)v - 1\end{aligned}$$

and *performance signal generator*[‡‡]

$$T_\pi \dot{w}_i = -w_i + (1+|u|^2)\begin{bmatrix} v^2 \\ 2v(\mu_i-\omega) \\ (\mu_i-\omega)^2 \end{bmatrix}, \quad i \in \mathcal{N} \tag{11}$$

where T_π is a positive constant no smaller then $1/\min\{R, 2\kappa\}$. For each pair $\{i, \eta\} \in \mathcal{N} \times \mathcal{T}$ we can then define a *performance signal*

$$\pi_{\{i,\eta\}} \triangleq \Pi(w_i, \eta) \tag{12}$$

where Π: $\mathbb{R}^3 \times \mathcal{T} \to \mathbb{R}$ denotes the *performance function* defined by

$$\Pi(w, \eta) = [\eta^2 \quad \eta \quad 1]\, w$$

The above definitions of the performance signal generator and performance function are prompted by the observation that, with the $\pi_{\{i,\eta\}}$ given by (12),

$$T_\pi \dot{\pi}_{\{i,\eta\}} = -\pi_{\{i,\eta\}} + (1+|u|^2)(\mu_i + \eta v - \omega)^2 \tag{13}$$

Now, it follows from (10) that $\tilde{\omega} = \mu_{i*} + \tau_{\mathrm{L}} v - \omega$. Therefore, since $1/T_\pi \leqslant \min\{R, 2\kappa\}$, Proposition 2.1 guarantees that for $\{i, \eta\} = \{i_*, \tau_{\mathrm{L}}\}$, $\pi_{\{i,\eta\}}$ converges to zero as fast as e^{-t/T_π}. Thus, each $\pi_{\{i,\eta\}}$ can be viewed as a measure of the expected performance of i and η as estimates of i_* and τ_{L}, respectively. In a supervisory control context, it is then natural to regard the pair[§§]

$$\{i_{\min}, \tau_{\mathrm{L}_{\min}}\} \triangleq \arg \min_{\{i,\eta\} \in \mathcal{N} \times \mathcal{T}} \pi_{\{i,\eta\}} = \arg \min_{\{i,\eta\} \in \mathcal{N} \times \mathcal{T}} \Pi(w_i, \eta) \tag{14}$$

as an estimate of $\{i_{i_*}, \tau_{\mathrm{L}}\}$. This is because the pair $\{i_{\min}, \tau_{\mathrm{L}_{\min}}\}$ is at least 'as good as' $\{i_{i_*}, \tau_{\mathrm{L}}\}$ as far as the values of the corresponding performance signals are concerned.

[‡‡] The first component of each of the w_i is generated by the same differential equation so the performance signal generator could be implemented more efficiently using a $(2N+1)$-dimensional system, instead of the $3N$-dimensional system in (11).

[§§] In general, the optimization in (14) can be computed in a closed form because, for each value of i, $\Pi(w_i, \eta)$ is a quadratic function of η.

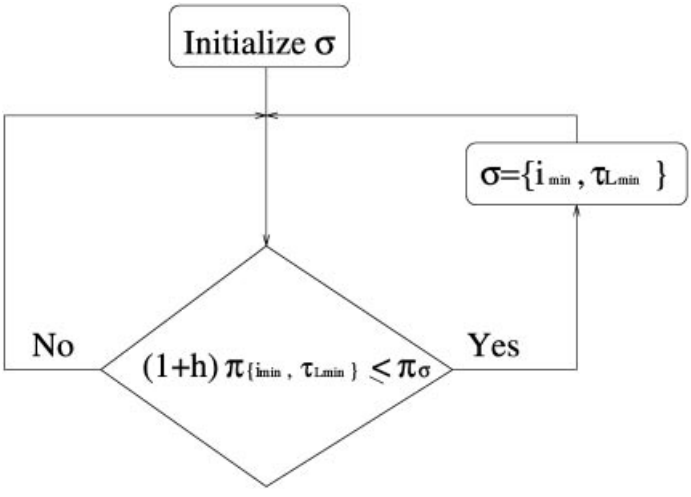

Figure 3. Scale-independent hysteresis switching logic.

The algorithm used to generate $\hat{R}$ is the *scale-independent hysteresis switching logic* [10] and can be regarded as the hybrid dynamical system, with state $\sigma \triangleq \{\sigma_1, \sigma_2\} \in \mathcal{N} \times \mathcal{T}$ and output

$$\hat{R} = R_{\sigma_1} \tag{15}$$

defined by the computer diagram in Figure 3. Here h is a pre-specified positive constant called the *hysteresis constant*, the $\pi_{\{i,\eta\}}$ are defined by (12), and the pair $\{i_{\min}, \tau_{L_{\min}}\}$ is defined by (14).

We shall require that the performance signal generator be initialized so that[¶¶]

$$\pi_{\{i,\eta\}}(0) > 0, \qquad \forall i \in \mathcal{N}, \eta \in \mathcal{T} \tag{16}$$

Because of (13), this guarantees that all the $\pi_{\{i,\eta\}}$ remain strictly positive for all future times. This is used in the sequel to exclude the possibility of chattering.

2.3. Summary

We regroup in this subsection all the equations describing the supervisor.

(i) A *multi-estimator* $\mathrm{E}: (u, \omega) \mapsto (\mu_1, \ldots, \mu_N, v)$ composed of N adaptive observers $\mathrm{E}_i(R_i)$, $i \in \mathcal{N}$ described by

$$\mathrm{E}_i(R_i): \quad \begin{cases} \dot{\lambda}_i = -R_i\lambda_i + R_i u \\ \dot{\mu}_i = -\kappa(1 + |u|^2)\mu_i + u^{\mathrm{T}} \mathcal{J} \lambda_i + \kappa(1 + |u|^2)\omega \\ \dot{v} = -\kappa(1 + |u|^2)v - 1 \end{cases} \tag{17}$$

where $\kappa > \frac{1}{2}$ and the R_i's are chosen from (3).

[¶¶] This can be achieved, for example, by setting $w_i(0) = [a, 2b, c]^{\mathrm{T}}$, $i \in \mathcal{N}$, for some $a, b, c \in \mathbb{R}$ so that $a > 0$ and $b^2 - ac < 0$.

(ii) A *performance signal generator* $\mathrm{PS}:(\mu_1,\ldots,\mu_N,v,\omega,u)\mapsto(\pi_{\{1,\eta\}},\ldots,\pi_{\{N,\eta\}})$ composed of N subsystems PS_i, $i\in\mathscr{N}$ of the form

$$T_\pi\dot{w}_i = -w_i + (1+|u|^2)\begin{bmatrix} v^2 \\ 2v(\mu_i-\omega) \\ (\mu_i-\omega)^2 \end{bmatrix} \tag{18}$$

$$\pi_{\{i,\eta\}} = [\eta^2 \quad \eta \quad 1]\,w_i$$

where $T_\pi > 0$ is a time constant that plays the role of a forgetting factor, as in standard adaptive control [16].

(iii) A *switching logic* S: $(\pi_{\{1,\eta\}},\ldots,\pi_{\{N,\eta\}})\mapsto\hat{R}$, with output $\hat{R}=R_{\sigma_1}$, which generates the estimate to be applied to the FOC according to the flow-graph of Figure 3. The hysteresis constant $h>0$ defines a relative threshold for the switching.

Besides the standard PI gains K_P, K_I of the FOC there are three more tuning gains in the proposed supervisory controller: κ, h and T_π. The gain κ determines the speed of convergence for the adaptive observers. High values of κ make the adaptive observers more rapid, but also more sensitive to measurement noise. As mentioned above, T_π acts as a forgetting factor in the evaluation of the performance signals, hence establishing a compromise between adaptation alertness and switching dither. The hysteresis threshold h, which is usually a very small number, has a similar effect in the transient performance. These issues will be illustrated with simulations in Section 4.

3. MAIN RESULT

Theorem 3.1

Assume that the set $\mathscr{T}$—to which τ_{L} is known to belong—is finite and consider the induction motor model (1) in closed-loop with the parameterized FOC (2), the multi-estimator (17), the performance signal generator (18), and the switching logic in Figure 3 with output given by (15). For any initialization of the closed-loop system such that (16) holds, the solution exists on $[0,\infty)$ and the signals $\lambda,\omega,v,\nu,\lambda_i,\mu_i,w_i,\ i\in\mathscr{N}$ are uniformly bounded on $[0,\infty)$. Moreover, ρ grows at most linearly with time and $\omega\to\omega_*$ as $t\to\infty$.

To prove Theorem 3.1. we need to introduce an auxiliary 'injected system'. To this effect, suppose that for a certain period of time the state σ of the switching logic is equal to some $q\triangleq\{k,\tau_{\mathrm{L}_k}\}$ in $\mathscr{N}\times\mathscr{T}$. Let

$$\hat{\omega}_k \triangleq \mu_k + \tau_{\mathrm{L}_k} v \tag{19}$$

be the corresponding ω-estimate and

$$\tilde{\omega}_k \triangleq \hat{\omega}_k - \omega \tag{20}$$

the corresponding estimation error. Using (20) to eliminate ω from Equations (2), (17), (15), one obtains

$$\begin{cases} \dot{v} = \hat{\omega}_k - \omega_* - \tilde{\omega}_k \\ \dot{\rho} = R_k \dfrac{\tau_d}{\beta_*^2} \\ \tau_d = -K_P(\hat{\omega}_k - \omega_* - \tilde{\omega}_k) - K_I v \\ u = \mathrm{e}^{\mathscr{J}\rho} \begin{bmatrix} \beta_* \\ \frac{\tau_d}{\beta_*} \end{bmatrix} \end{cases} \tag{21}$$

and

$$\begin{cases} \dot{\lambda}_i = -R_i\lambda_i + R_i u, & i \in \mathscr{N} \\ \dot{\mu}_i = -\kappa(1+|u|^2)\mu_i + u^{\mathrm{T}}\mathscr{J}\lambda_i + \kappa(1+|u|^2)(\hat{\omega}_k - \tilde{\omega}_k), & i \in \mathscr{N} \\ \dot{v} = -\kappa(1+|u|^2)v - 1 \end{cases} \tag{22}$$

Equations (19), (21), and (22) can be regarded as a dynamical system—often called the *qth injected system*—whose input is the estimation error $\tilde{\omega}_k$ and whose state consists of the combined states of the parameterized FOC and the multi-estimator [9].

Suppose for a moment that $\tilde{\omega}_k = 0$. In view of (19) and (22)

$$\dot{\lambda}_k = -R_k\lambda_k + R_k u, \quad \dot{\hat{\omega}}_k = u^{\mathrm{T}}\mathscr{J}\lambda_k - \tau_{\mathrm{L}_k}$$

thus $\{\lambda_k, \omega_k\}$ could be regarded as the state of an induction motor model with rotor resistance R_k and load torque τ_{L_k}. It is therefore not surprising that the interconnection of these equations with the FOC (21)—which was designed for a rotor resistance equal to R_k—results in a stable system. One could then conclude that all signals would be bounded if $\tilde{\omega}_k = 0$. When $\tilde{\omega}_k \neq 0$, boundedness is still preserved provided that $\tilde{\omega}_k$ is well behaved. The following lemma, which is proved in the Appendix, formalizes this observation.

Lemma 3.2

Consider the qth injected system defined by (19), (21), and (22). Given an interval $[t_0, T)$ (with $t_0 \geqslant 0$ and $T \in (t_0, +\infty]$) and any piecewise continuous signal $\tilde{\omega}_k$ for which

$$\int_{t_0}^{T} \tilde{\omega}_k^2(\tau)\,\mathrm{d}\tau < \infty \quad \text{and} \quad \int_{t_0}^{T} |u(\tau)|^2\tilde{\omega}_k^2(\tau)\,\mathrm{d}\tau < \infty$$

the signals v, ν, λ_i, μ_i, $i \in \mathscr{N}$ are uniformly bounded on $[t_0, T)$ and ρ grows, at most, linearly with time.[‖] Moreover, if $T = +\infty$ then $\hat{\omega}_k \to \omega_*$, $|\lambda_k| \to \beta_*$, and $v \to -\tau_{\mathrm{L}_k}/K_I$ as $t \to \infty$.

We can now proceed with the proof of Theorem 3.1. For any piecewise-constant signal $s\colon [0, \infty) \to \mathscr{N} \times \mathscr{T}$ and any initialization of the system defined by (1), (2), (17)–(18), and (15), with

[‖] Thus ρ is also uniformly bounded on $[0, T)$ if $T < \infty$.

$\sigma = s$, it follows from Proposition 2.1 that

$$e^{T_s/T_\pi}\pi_{\{i_*,\tau_L\}}(T_s) < \infty$$

where $[0, T_s)$ is the interval of maximal length on which the solution exists. Therefore, if we define the *scaled performance signals*

$$\bar{\pi}_{\{i,\eta\}}(t) \triangleq e^{t/T_\pi}\pi_{\{i,\eta\}}(t), \quad \{i, \eta\} \in \mathcal{N} \times \mathcal{T} \tag{23}$$

then (i) $\bar{\pi}_{\{i_*,\tau_L\}}$ is bounded on $[0, T_s)$. Moreover, because of (13) and (16),

$$\dot{\bar{\pi}}_{\{i,\eta\}} = \frac{e^{t/T_\pi}}{T_\pi}(1 + |u|^2)(\mu_i + \eta v - \omega)^2, \quad \bar{\pi}_{\{i,\eta\}}(0) > 0, \quad \{i, \eta\} \in \mathcal{N} \times \mathcal{T}$$

thus we also conclude that (ii) each $\bar{\pi}_{\{i,\eta\}}$ is positive and has a limit as $t \to T_s$. This is because each $\bar{\pi}_{\{i,\eta\}}$ is a non-decreasing functions of t that starts positive. In the sequel we make use of the above properties (i) and (ii).

The interconnected system defined by (1), (2), (17)–(18), (15) is a dynamical system of the form

$$\dot{z} = f_\sigma(z), \quad \pi_{\{i,\eta\}} = g_{\{i,\eta\}}(z), \quad \{i, \eta\} \in \mathcal{N} \times \mathcal{T} \tag{24}$$

where $z \triangleq \{\lambda, \omega, v, \rho, \nu, \lambda_i, \mu_i, w_i : i \in \mathcal{N}\}$ and, for each $\{i, \eta\} \in \mathcal{N} \times \mathcal{T}$, $f_{\{i,\eta\}}$ and $g_{\{i,\eta\}}$ are locally Lipschitz. Because of the hysteresis constant h, for each initial state $\{z(0); \sigma(0)\}$ for which (16) holds, there must be an interval $[0, T)$ of maximal length on which there is a unique pair $\{z; \sigma\}$ with z continuous and σ piecewise constant, which satisfies (24) when σ is generated by the scale-independent hysteresis switching logic [10]. Moreover, on each proper subinterval $[0, \tau) \subset [0, T)$, σ can switch at most a finite number of times.

The term 'scale-independence' is prompted by the fact that if θ is any piecewise continuous signal which is positive on $[0, \infty)$, the state σ of the switching logic remains unchanged if each performance signal $\pi_{\{i,\eta\}}$, $\{i, \eta\} \in \mathcal{N} \times \mathcal{T}$ is replaced $\theta\pi_{\{i,\eta\}}$. Thus, because of (23), and as far as the signal σ is concerned, we can think of the switching logic as being driven by the scaled performance signals $\bar{\pi}_{\{i,\eta\}} = \theta\pi_{\{i,\eta\}}$, with $\theta(t) = e^{t/T_\pi}$, $t \geqslant 0$. The fact that the $\bar{\pi}_{\{i,\eta\}}$ possess properties (i) and (ii) noted above, enable us to exploit the scale-independent hysteresis switching lemma [10] and consequently to draw the following conclusion.

Lemma 3.3

For an arbitrary initialization of the closed-loop system such that (16) holds, let $\{\sigma, \lambda, \omega, v, \rho, \nu, \lambda_i, \mu_i, w_i : i \in \mathcal{N}\}$ denote the unique solution to (1), (2), (17)–(18), (15) with σ generated by switching logic in Figure 3. If $[0, T)$ is the largest interval on which this solution is defined, there is a time $T^* < T$ beyond which σ is constant and $e^{t/T_\pi}\pi_{\sigma(T^*)}(t)$ is bounded on $[0, T)$.

Let $\sigma, \lambda, \omega, v, \rho, \nu, \lambda_i, \mu_i, w_i$, $(i \in \mathcal{N})$, T, and T^* be as in Lemma 3.3 and set $\{k, \tau_{L_k}\} \triangleq \sigma(T^*)$. Because of (13) and the observation that $e^{t/T_\pi}\pi_{\sigma(T^*)}(t)$ is bounded on $[0, T)$, one concludes that

$$\frac{1}{T_\pi}\int_{T^*}^{T} e^{\tau/T_\pi}(1 + |u(\tau)|^2)\,\tilde{\omega}_k^2(\tau)\,d\tau < \infty \tag{25}$$

with

$$\tilde{\omega}_k \triangleq \hat{\omega}_k - \omega, \quad \hat{\omega}_k \triangleq \mu_i + \tau_{\mathrm{L}_k} v \tag{26}$$

Since σ is frozen at $\{k, \tau_{\mathrm{L}_k}\}$ for $t \in [T^*, T)$ and (25) holds, Lemma 3.2 (with $t_0 \triangleq T^*$) allows one to conclude that the combined state of the parameterized FOC and the multi-estimator is bounded on $[T^*, T)$, except for $\rho(t)$ that grows linearly with t. Now, in view of Proposition 2.1, we also know that

$$|\omega(t) - \mu_{i_*}(t) - \tau_{\mathrm{L}} v(t)| < \infty, \quad |\lambda(t) - \lambda_{i_*}(t)| < \infty$$

Thus, since μ_{i_*}, v, and λ_{i_*} are bounded on $[T^*, T)$, so are ω and λ. From this and (18) one further concludes that all the w_i are bounded on $[T^*, T)$.

Now if T were finite, the solution to (1), (2), (17)–(18), (15) could be continued onto at least an open half interval of the form $[T, T_1)$ thereby contradicting the hypothesis that $[0, T)$ is the system's interval of maximal existence. By contradiction one can therefore conclude that $T = \infty$ and that the signals λ, ω, v,v, λ_i, μ_i, w_i, $i \in \mathcal{N}$ are uniformly bounded on $[0, \infty)$.

With global existence of solution established, Lemma 3.2 allows one to further conclude that $\lim_{t\to\infty} \hat{\omega}_k = \omega_*$. Now $\lim_{t\to\infty} \tilde{\omega}_k = 0$ because $\tilde{\omega}_k^2 \in \mathscr{L}^1[0, \infty)$ and $(\mathrm{d}/\mathrm{d}t)\tilde{\omega}_k{}^2$ is bounded on $[0, \infty)$ (cf. [17, Lemma 1, p. 58]). From this and (26) it follows that $\lim_{t\to\infty} \omega = \lim_{t\to\infty} \hat{\omega}_k = \omega_*$.

4. SIMULATIONS

With the goal of verifying the performance of the supervisor FOC described above several simulation tests were carried out. We consider first the academic example reported in Reference [5], then we test our algorithm in the benchmark problem studied in Reference [18]. Some experimental results for the latter may be found in Reference [19].

4.1. Academic example

In the example of Reference [5] the (fixed parameter) FOC operates very close to the stability boundary predicted in proposition 4 of Reference [1], and a small change in the rotor resistance drives the system to instability. This is illustrated in Figure 4 where we have set $K_P = 0.1$, $K_I = 1$, $\beta_* = 1$, $\omega_* = 10$, $\hat{R} = 10$, the initial conditions are all set equal to zero except $\omega(0) = 10.1$ and the motor operates without load, i.e. $\tau_{\mathrm{L}} = 0$. The rotor resistance changes from its initial value $R = 6$, for which the closed-loop is stable, to the instability region of $R = 4$ at $t = 40$. The theoretical stability/instability boundary in this case is $R = 4.9$. Figure 5 shows the same experiment but with the supervisory FOC with $N = 6$, $\mathscr{R} = \{2, 4, \ldots, 12\}$, $\sigma_2(0) = 0.5$ (note: $\sigma_2(0)$ is the initial estimate for τ_{L}) , $\hat{R}(0) = 10$ and $\kappa = 5$, $h = 0.02$, $T_\pi = 1/3.5$. For the extreme points of the interval, to which the load torque τ_{L} belongs, we have fixed $\tau_{\mathrm{L}m} = 0$ and $\tau_{\mathrm{L}M} = 5$. The initial conditions of w_i were chosen so that (16) holds. Their initial values were $w_i(0) = [2, -2, 2]^{\mathrm{T}}$ for $i \in \mathcal{N}$. Notice that, after a very brief transient, the supervisor correctly estimates the resistance value and stabilizes the motor.

With the goal of testing the sensitivity of the proposed scheme to the discrete set of resistance values, we simulated the case where the real value of the rotor resistance does not match any of

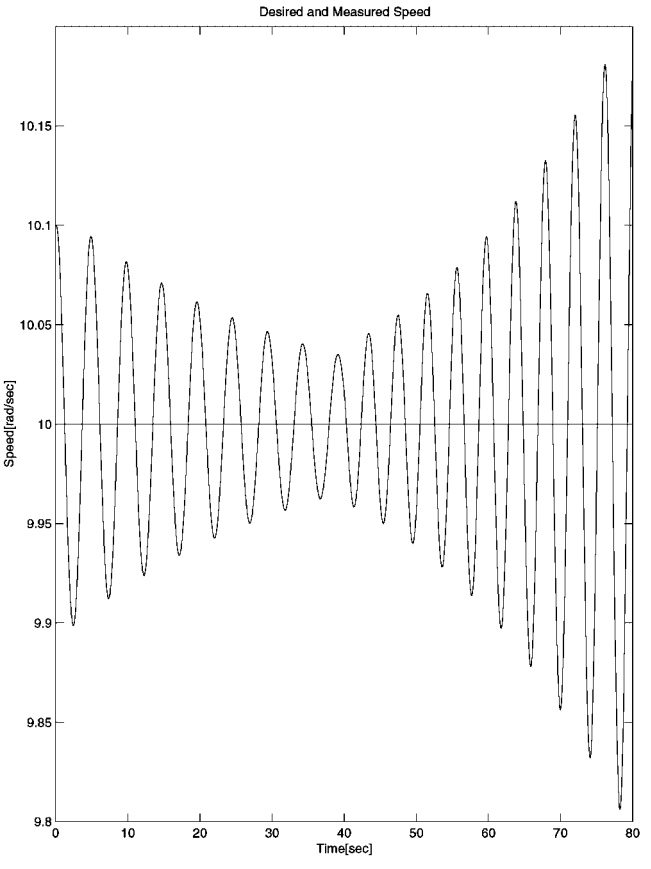

Figure 4. Instability in the non-adaptive FOC due to a change in the rotor resistance.

the values of the discrete set $\mathscr{R}$. The simulation is the same as above except for the real rotor resistance that changes from its initial value $R = 6$ to $R = 3.8$ at $t = 40$, instead of $R = 4$. This is illustrated in Figure 6, where we can see that the estimator chooses the value of the discrete set that is the closest to the real value.

In a third test, we considered a situation where both the rotor resistance and the load torque change. The rotor resistance changes from its initial value $R = 6$ to 8 at $t = 60$ and the load torque changes from its initial value $\tau_L = 2$ to 3 at $t = 20$ and changes again to $\tau_L = 4$ at $t = 40$. From Figure 7, one can observe that the tracking as well as the correct estimation of the rotor resistance and the load torque are achieved with only brief burstings at the jump instants.

Finally, we investigated the sensitivity of the algorithm *vis-à-vis* the filter time constant T_π. For this, we repeated the simulation of Figure 5 (with the difference of having set $\tau_L = 2$ instead of $\tau_L = 0$), changing the value of T_π. Figure 8 shows that, as expected due to a longer memory in the performance signals, when the value of T_π is increased (in this case to 1/0.35), the transient becomes much slower. On the other hand, if we set T_π to a very small value (1/100 in Figure 9) the switching is faster but exhibits significant dither.

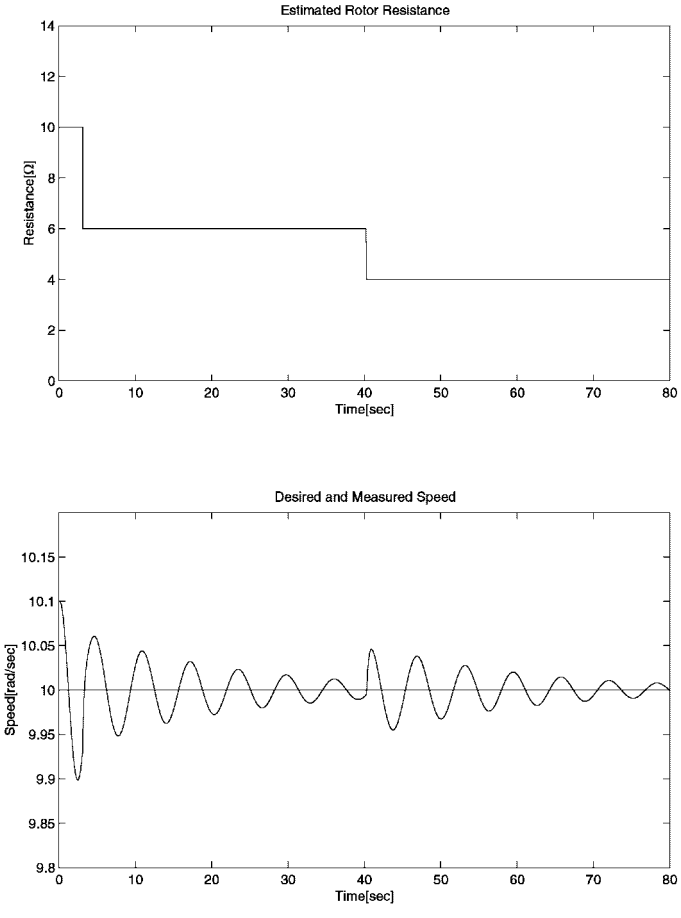

Figure 5. Stabilization with supervisory FOC.

Other simulations with various values of κ and h confirmed that performance is less sensitive to these parameters, and their effect is as predicted in Section 2.3.

4.2. Benchmark problem

The benchmark problem proposed in Reference [18] included some reference tracking experiments with time–varying rotor resistance and step changes in the load torque for a motor with the specifications given in the Table I.

In Figure 10 we show the performance of the estimators of load torque and rotor resistance with the following control parameters and test conditions: $K_P = 0.5$, $K_I = 0.3$, $h = 0.45$, $\kappa = 12$, $T_\pi = 0.1$, $\mathscr{R} = \{4, 6, 8\}$ and $\tau_L = \pm 3.6$ N m. Notice that the supervisor correctly estimates the resistance value and the load torque. The speed error, which is not shown here, is kept within practically reasonable bounds. The gains K_P and K_I were selected following the tuning procedure

Table I. System parameters of induction motors.

Motor description	Notation	Value	Unit
Rated power	P^N	1.1	KW
Rated torque	τ^N	7	Nm
Power factor	$\cos(\phi)$	0.83	
Number of pole-pairs	n_p	2	
Rated speed	w_r^N	73.3	rad/sec
Rated rotor flux norm	β_*^N	1.14	Wb
Stator resistance	R_s	8	Ohm
Rotor resistance	R_r	4	Ohm
Stator inductance	L_s	0.47	H
Rotor inductance	L_r	0.47	H
Mutual inductance	L_{sr}	0.44	H
Total leakage factor($\sigma_r + \sigma_s = 2 \times 0.06$)	σ	0.12	
Shaft inertia moment	J	0.015	$Kg - m^2$
Inverter description			
Rated stator voltage	$\|\|U_s\|\|$	210	V
Rated stator current	$\|\|I_s\|\|$	12	A
Sampling frequency	f_{sl}	13	kHz

of Reference [5]. The initial conditions are all set equal to zero except $\hat{R}(0) = 4$ and $w_i(0) = [2, -2, 2]^T$ for $i \in \{1, 2, 3\}$.

In a second test, we investigated the sensitivity of the algorithm *vis-à-vis* the hysteresis threshold h, and the filter time constant T_π. To this end, we repeated the simulation of Figure 10 changing the corresponding parameters as indicated in Figures 11 and 12. As expected, there is a clear tradeoff between alertness of the estimator and transient behavior. We also tested the robustness of the scheme with respect to uncertainty to other motor parameters, e.g. the inertia J, showing that it is quite insensitive.

5. CONCLUSIONS

We have presented in this paper an application of supervisory control to induction motors with uncertainty in the rotor resistance. This is a problem of great practical importance which, in the authors' opinion, had not found a satisfactory solution in the literature. Motivated by industrial practice we consider the case of current-fed induction motors and propose to adjust on-line one parameter of the existing FOC. The overall algorithm is shown to be globally convergent under the assumption that the actual rotor resistance belongs to a given discrete set and that the load torque ranges in some known finite set. Both assumptions are reasonable in applications. The assumption that τ_L belongs to a *finite* set $\mathscr{T}$ is of technical nature. The simulation results indicate that the algorithm performs well even when $\mathscr{T}$ is an interval. We should remark that we can take a very fine grid for $\mathscr{T}$ without increasing the computational burden.

In spite of its apparent complexity the supervisor involves very simple operations, which can be easily implemented in modern DSPs with numerically robust algorithms. The performance of the algorithm, as well as its sensitivity to the various tuning parameters, were tested via simulations both in an academic example and in a benchmark problem recently proposed in the literature.

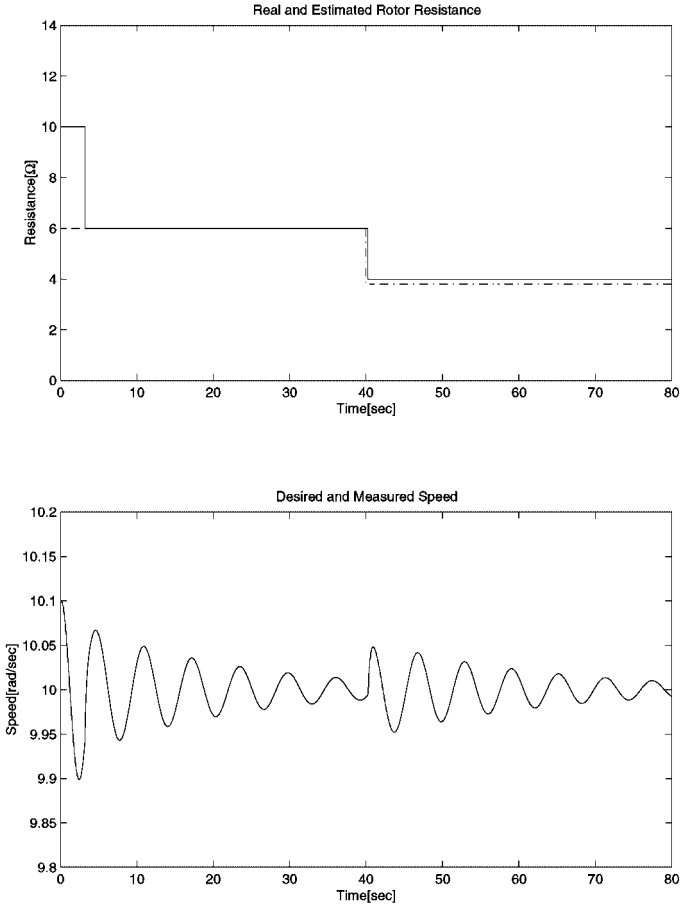

Figure 6. Sensitivity to the discrete set of resistance values. (- . -) Real rotor resistance (—) Estimated rotor resistance.

APPENDIX A

Proof of Lemma 3.2. Defining,

$$e_v \triangleq v + \frac{\tau_{L_k}}{K_I}, \qquad e_{\omega_k} \triangleq \hat{\omega}_k - \omega_*, \qquad e_{\lambda_k} \triangleq \lambda_k - \lambda_d$$

with $\lambda_d \triangleq \beta_* \begin{bmatrix} \cos\rho \\ \sin\rho \end{bmatrix}$, from (19), (21), and (22) one concludes that

$$\dot{e}_{\lambda_k} = -R_k e_{\lambda_k} \tag{A1}$$

$$\dot{e}_v = e_{\omega_k} + \left(\frac{\gamma}{K_I} - 1\right)\tilde{\omega}_k \tag{A2}$$

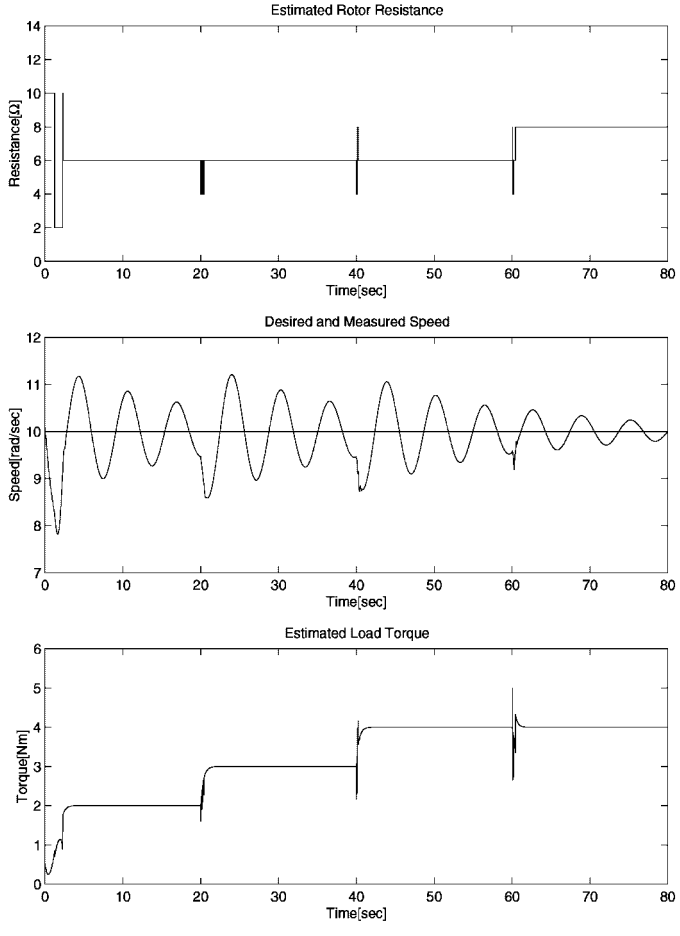

Figure 7. Simultaneous change of rotor resistance and load torque.

$$\dot{e}_{\omega_k} = \lambda_d^{\mathrm{T}} \mathcal{J} e_{\lambda_k} + \left(1 + \frac{\lambda_d^{\mathrm{T}} e_{\lambda_k}}{\beta_*^2}\right) \tau_d - \tau_{\mathrm{L}_k} - \kappa(1 + |u|^2)\, \tilde{\omega}_k \tag{A3}$$

$$\tau_d = -K_P e_{\omega_k} - K_I e_v + \tau_{\mathrm{L}_k} + K_P\, \tilde{\omega}_k \tag{A4}$$

$$\tilde{\omega}_k |u|^2 = \tilde{\omega}_k\, u' \left(\lambda_d + \frac{1}{\beta_*^2}\, \mathcal{J} \lambda_d \tau_d\right) \tag{A5}$$

Replacing (A4)–(A5) in (A3) yields

$$\dot{e}_{\omega_k} = -\left(1 + \frac{\lambda_d^{\mathrm{T}} e_{\lambda_k}}{\beta_*^2} - \tilde{\omega}_k\, u' \frac{1}{\beta_*^2}\, \mathcal{J} \lambda_d\right)(K_P e_{\omega_k} + K_I e_v) + \lambda_d^{\mathrm{T}} \left(\mathcal{J} + \frac{\tau_{\mathrm{L}_k}}{\beta_*^2} I\right) e_{\lambda_k}$$

$$+ K_P \left(1 + \frac{\lambda_d^{\mathrm{T}} e_{\lambda_k}}{\beta_*^2} - \kappa\right) \tilde{\omega}_k - \lambda_d' \left(I - \frac{\tau_{\mathrm{L}_k}}{\beta_*^2}\, \mathcal{J}\right) u \tilde{\omega}_k + K_P\, \frac{1}{\beta_*^2}\, \lambda_d'\, \mathcal{J} u \tilde{\omega}_k^2 \tag{A6}$$

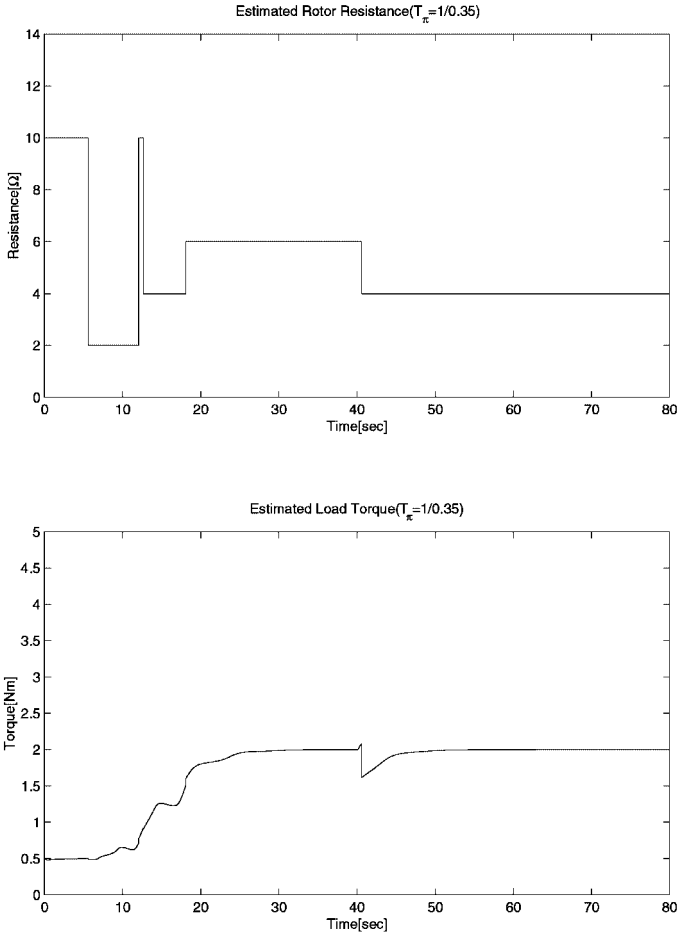

Figure 8. Sensitivity with respect to T_π.

Thus one can write (A2) and (A6) as

$$\dot{x} = (A + \tilde{\omega}_k u' \bar{A})\, x + b_1 e_{\lambda_k} + b_2 \tilde{\omega}_k + B_3 u \tilde{\omega}_k + B_4 u \tilde{\omega}_k^2 \tag{A7}$$

where $x \triangleq [e_v \;\; e_{\omega_k}]'$ and $A, \bar{A}, b_1, b_2, B_3, B_4$ are appropriately defined time-varying uniformly bounded matrices with A converging exponentially fast to the asymptotically stable matrix $\left[\begin{smallmatrix} 0 & 1 \\ -K_I & -K_P \end{smallmatrix}\right]$. This is because λ_d is uniformly bounded and e_{λ_k} converges to zero exponentially fast. The fact that $A + \tilde{\omega}_k u' \bar{A}$ differs from an exponentially stable matrix by an $\mathscr{L}^2$ perturbation guarantees that $A + \tilde{\omega}_k u' \bar{A}$ is still exponentially stable [20]. Thus (A7) can be regarded as an exponentially stable linear time-varying system whose inputs e_{λ_k}, $\tilde{\omega}_k$, and $u\tilde{\omega}_k$ are in $\mathscr{L}^2[t_0, T)$ and the input $u\tilde{\omega}_k^2$ is in $\mathscr{L}^1[t_0, T)$ (note that $|u\tilde{\omega}_k^2| \leqslant \frac{1}{2}|u\tilde{\omega}_k|^2 + \frac{1}{2}\tilde{\omega}_k^2$). This allows one to conclude that x must be uniformly bounded on $[t_0, T)$ and, if $T = +\infty$, we also have that $\lim_{t \to \infty} x = 0$.

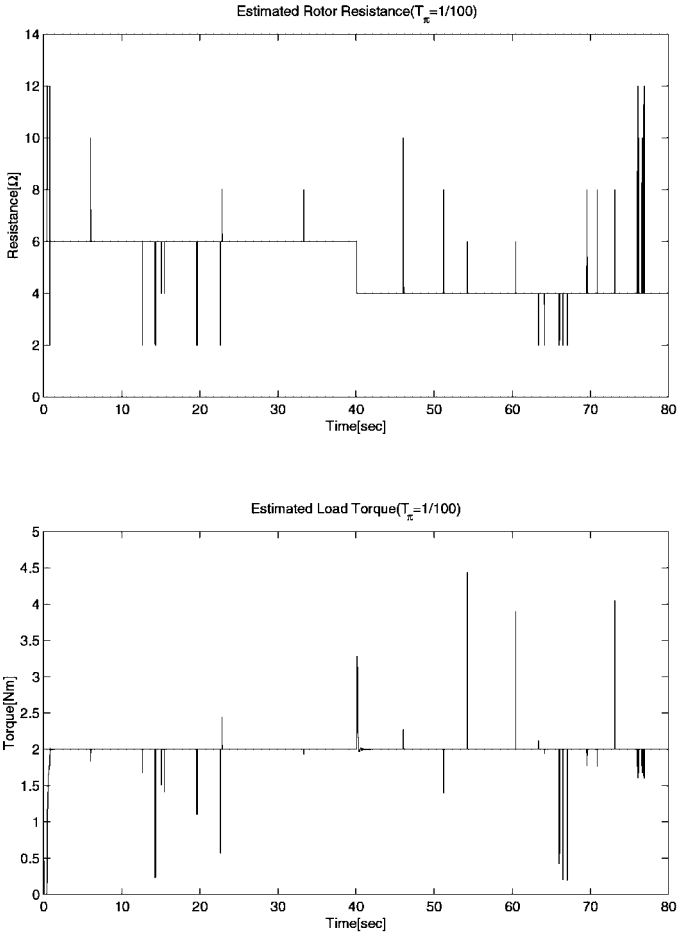

Figure 9. Sensitivity with respect to T_π.

The latter implying that $\lim_{t\to\infty}\hat{\omega}_k = \omega_*$ and $\lim_{t\to\infty} v = -\tau_{L_k}/K_I$. Note also that (A1) implies that $\lim_{t\to\infty}|\lambda_k - \lambda_d| = 0$ and therefore that $\lim_{t\to\infty}|\lambda_k| = |\lambda_d| = \beta_*$.

Now uniform boundedness of x guarantees uniform boundedness of v and $\hat{\omega}_k$ but it still remains to show that the remaining signals are bounded. To this effect note that from (21) and (A4) one concludes that

$$u = u_1 + u_2$$

with

$$u_1 \triangleq \left(I + \frac{\tau_{L_k}}{\beta_*^2}\,\mathcal{J}\right)\lambda_d - \frac{1}{\beta_*^2}\,\mathcal{J}\lambda_d(K_P e_{\omega_k} + K_I e_v), \qquad u_2 \triangleq \frac{K_P}{\beta_*^2}\,\mathcal{J}\lambda_d\tilde{\omega}_k$$

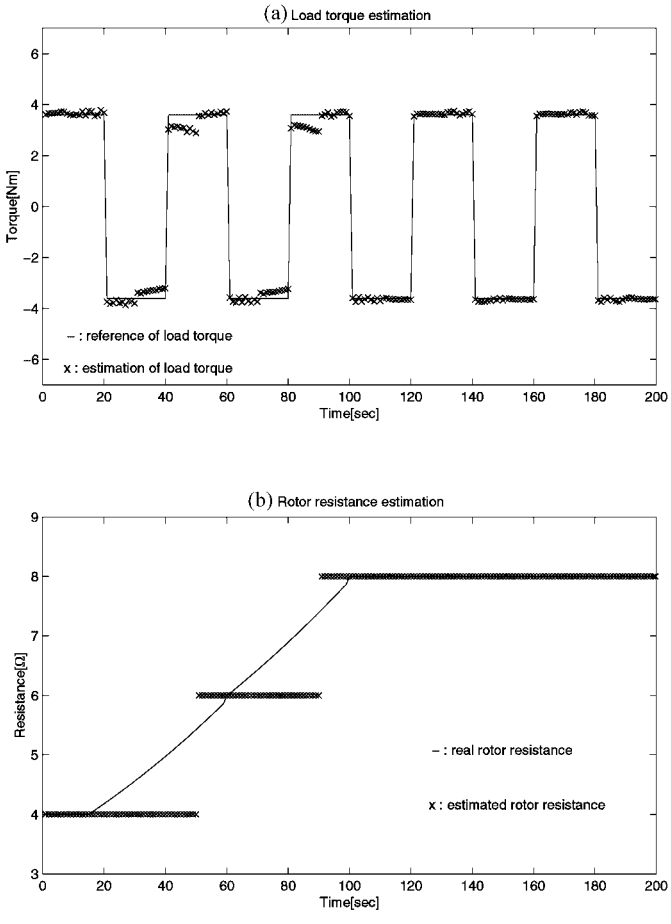

Figure 10. Load torque and rotor resistance estimation.

Since λ_d and x are uniformly bounded, u_1 is also uniformly bounded and since $\tilde{\omega}_k$ is in $\mathscr{L}^2[t_0, \infty)$, u_2 is also in $\mathscr{L}^2[t_0, T)$. Thus all the λ_i ($i \in \mathscr{N}$) are uniformly bounded because these signals are generated by stable linear systems with input $u = u_1 + u_2$ with u_1 bounded and $u_2 \in \mathscr{L}^2[t_0, T)$. A similar reasoning can also be used to conclude that v and all the μ_i are uniformly bounded.

Regarding the boundedness of ρ, from (21) and (A4), one concludes that

$$\rho(t) = \rho(0) + \frac{R_k}{\beta_*^2} \int_0^t \tau_d(\tau)\, \mathrm{d}\tau$$

$$\leqslant \rho(0) + \frac{R_k}{2\beta_*^2} \int_0^t (|\tau_{\mathbf{L}_k} - K_P e_{\omega_k} - K_I e_v| + K_P|\tilde{\omega}_k|)\, \mathrm{d}\tau$$

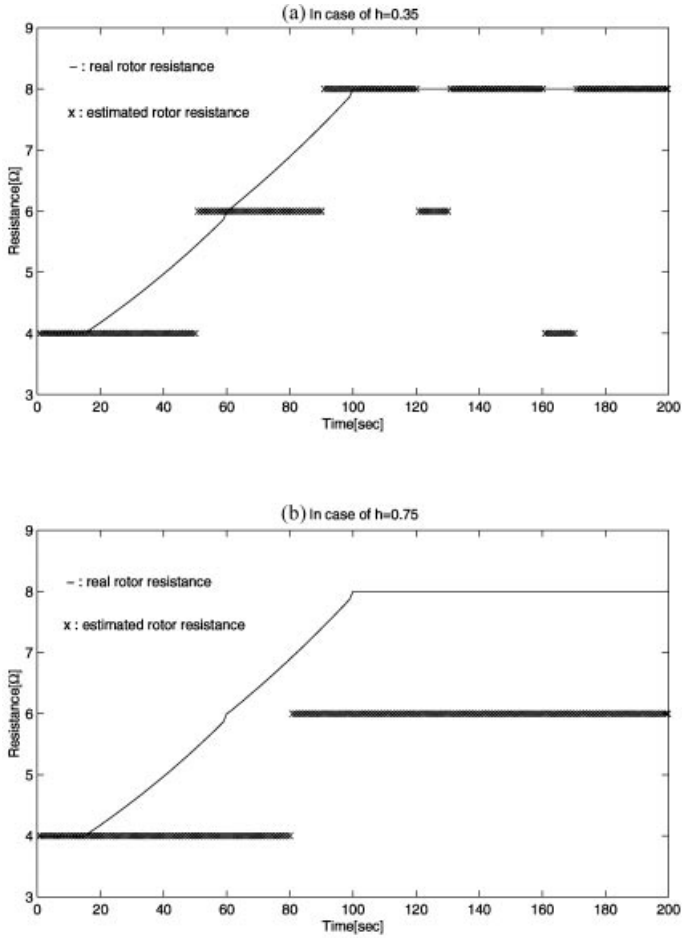

Figure 11. Sensitivity of the resistance estimator with respect to h.

$$\leqslant \rho(0) + \frac{R_k}{2\beta_*^2} \int_0^t \left(|\tau_{L_k} - K_P e_{\omega_k} - K_I e_v| + \frac{K_P}{2} + \frac{K_P}{2} \tilde{\omega}_k^2 \right) \mathrm{d}\tau$$

Here we used Schwartz inequality. Since it has been established that e_{ω_k} and e_v are bounded and $\tilde{\omega}_k \in \mathscr{L}^2[t_0, T)$, one concludes that $\rho(t)$ grows at most linearly with t. ■

ACKNOWLEDGEMENTS

The work of M. Netto is sponsored by the Brazilian foundation CAPES.

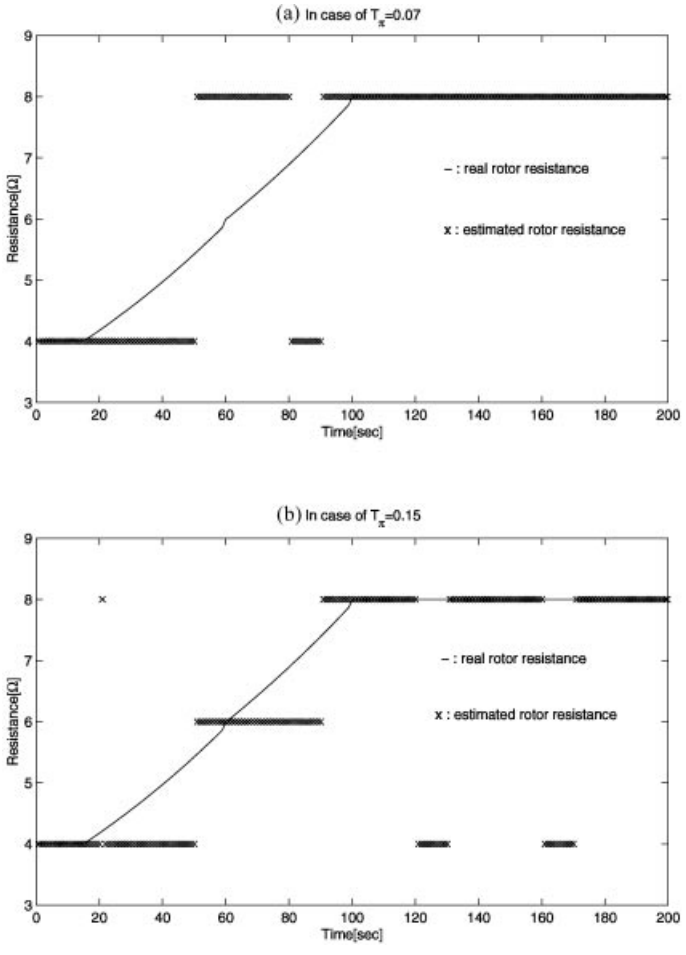

Figure 12. Sensitivity of the resistance estimator with respect to T_π.

REFERENCES

1. de Wit P, Ortega R, Mareels I. Indirect field-oriented control of induction motors is robustly globally stable. *Automatica* 1996; **32**(10):1393–1402.
2. Ortega R, Loria A, Nicklasson PJ, Sira-Ramirez H. *Passivity-Based Control of Euler-Lagrange Systems*, Communications and Control Engineering. Springer: Berlin, 1998.
3. Kim K, Ortega R, Charara A, Vilain J. Theoretical and experimental comparison of two nonlinear controllers for current-fed induction motors. *IEEE Transactions on Control Systems and Technology*, 1997; **5**(3):1–11.
4. Taoutaou D, Puerto R, Ortega R, Loron L. A new field-oriented discrete-time controller for current-fed induction motors. *Control Engineering Practice* 1997; **5**(2):209–217.
5. Chang GW, Espinosa G, Mendes E, Ortega R. On FOC of induction motors: tuning of the PI gains for performance enhancement. *IEEE Transactions on Industrial Electronics* 2000; **47**(3).
6. Morse AS. Supervisory control of families of linear set-point controllers – Part 1: exact matching. *IEEE Transactions on Automatic Control* 1996; **41**(10).
7. Morse AS. Supervisory control of families of linear set-point controllers – Part 2: robustness. *IEEE Transactions on Automatic Control* 1997; **42**(11).

8. Morse AS. Towards a unified theory of adaptive control—Part II: certainty equivalence and implicit tuning. *IEEE Transactions on Automatic Control* 1992; **37**(1):15–29.
9. Hespanha JP, Morse AS. Certainty equivalence implies detectability. *Systems & Control Letters* 1999; **36**(1):1–13.
10. Hespanha JP. Logic-based switching algorithms in control. *Ph.D. Thesis*, Yale University, USA, December 1998.
11. Garces LJ. Parameter adaptation for the speed controlled static AC drive with a squirrel-cage induction motor. *IEEE Transactions on Industrial Applications* 1980; **16**:173–178.
12. Marino R, Peresada S, Tomei P. Output-feedback control of current-fed induction motors with unknown rotor resistance. *IEEE Transactions on Control and Systems Technology* July 1996; **4**(4).
13. Ahmed-Ali T, Lamnabhi-Lagarrigue F, Ortega R. A globally-stable adaptive field-oriented controller for current-fed induction motors. *International Journal of Control* 1999; **72**(11):996–1005.
14. Marino R, Peresada S, Tomei P. Global adaptive output-feedback control of induction motors with uncertain rotor resistance. *IEEE Transactions on Automatic Control* 1999; **44**(5):2190–2194.
15. Vedagarbha P, Dawson DM, Burg T. Nonlinear control of induction motors: the observed field oriented control scheme. *Proceedings of the 35th IEEE CDC*, Kobe, Japan, December 1996; 4707–4712.
16. Sastry S, Bodson M. *Adaptive Control: Stability, Convergence and Robustness*. Prentice-Hall: Englewood Cliffs, NJ, 1989.
17. Aizerman MA, Gantmacher FR. *Absolute Stability of Regulator Systems*. Holden-Day: San Francisco, CA, 1964.
18. Ortega R, Asher G, Mendes E (Eds). Special issue on nonlinear control of induction motors. *International Journal on Adaptive Control and Signal Processing* 2000; **14**(2/3).
19. Chang GW. On the nonlinear control of electrical machines: synchronous and induction motors. *Ph.D. Thesis*, September 1999, LSS–Supelec, France.
20. Bellman R. *Stability Theory of Differential Equations*. Dover Publications: New York, 1969.

